2. REPORT DATE	3. REPORT TYPE AND DATES COVERED
Nov 12, 1992	Reprint

4. TITLE AND SUBTITLE
On the Evidence for Mesogranules in Solar Power Spectra

5. FUNDING NUMBERS
PE 61102F
PR 2311
TA G3
WU 27

(2)

6. AUTHOR(S)
Gregory P. Ginet, George W. Simon

7. PERFORMING ORGANIZATION NAME(S) AND ADDRESS(ES)
Phillips Lab/GPSS
Hanscom AFB
Massachusetts 01731-5000

8. PERFORMING ORGANIZATION REPORT NUMBER
PL-TR-92-2298

9. SPONSORING/MONITORING AGENCY NAME(S) AND ADDRESS(ES)

10. SPONSORING/MONITORING AGENCY REPORT NUMBER

11. SUPPLEMENTARY NOTES
Reprinted from The Astrophysical Journal 386: 359-363, 1992 February 10

12a. DISTRIBUTION/AVAILABILITY STATEMENT
Approved for public release; Distribution unlimited

12b. DISTRIBUTION CODE

13. ABSTRACT (*Maximum 200 words*)

The power spectrum of the horizontal component of the solar convective velocity field has recently been estimated from observations of the Doppler shifts of surface flows at and near disk center (Chou et al.). From their analysis, the authors assert that "there is no evidence of apparent energy excess at the scale of mesogranulation." We show in this paper that their conclusion is incorrect and that the shape of the observational spectrum does indeed confirm the presence of both supergranules and mesogranules in the solar convective flow.

To establish this claim we have extended existing kinematic models of convection at the solar surface (Simon and Weiss; Simon et al.) and have introduced power spectra diagnostics. We find that models with supergranule cells alone do not produce spectra that match the observations, but if mesogranules are included then there is excellent agreement between the model and observational spectra when the model parameters are chosen to be consistent with proper motion and Doppler measurements. Since the magnitudes of our model spectra are consistent with earlier Doppler measurements of the rms horizontal velocity field, but are significantly less than those of the observed spectrum, we must call into question the analysis of Chou et al.

14. SUBJECT TERMS
Convection -Sun: granulation

15. NUMBER OF PAGES
5

16. PRICE CODE

17. SECURITY CLASSIFICATION OF REPORT	18. SECURITY CLASSIFICATION OF THIS PAGE	19. SECURITY CLASSIFICATION OF ABSTRACT	20. LIMITATION OF ABSTRACT
Unclassified	Unclassified	Unclassified	SAR

THE ASTROPHYSICAL JOURNAL, 386:359–363, 1992 February 10

ON THE EVIDENCE FOR MESOGRANULES IN SOLAR POWER SPECTRA

GREGORY P. GINET
Phillips Laboratory (AFSC), GP/PHG, Hanscom AFB, MA 01731

AND

GEORGE W. SIMON
Phillips Laboratory (AFSC), National Solar Observatory/Sacramento Peak,[1] Sunspot, NM 88349
Received 1991 July 9; accepted 1991 August 12

ABSTRACT

The power spectrum of the horizontal component of the solar convective velocity field has recently been estimated from observations of the Doppler shifts of surface flows at and near disk center (Chou et al.). From their analysis, the authors assert that "there is no evidence of apparent energy excess at the scale of mesogranulation." We show in this paper that their conclusion is incorrect and that the shape of the observational spectrum does indeed confirm the presence of both supergranules and mesogranules in the solar convective flow.

To establish this claim we have extended existing kinematic models of convection at the solar surface (Simon and Weiss; Simon et al.) and have introduced power spectra diagnostics. We find that models with supergranule cells alone do not produce spectra that match the observations, but if mesogranules are included then there is excellent agreement between the model and observational spectra when the model parameters are chosen to be consistent with proper motion and Doppler measurements. Since the magnitudes of our model spectra are consistent with earlier Doppler measurements of the rms horizontal velocity field, but are significantly less than those of the observed spectrum, we must call into question the analysis of Chou et al.

Subject headings: convection — Sun: granulation

1. INTRODUCTION

With the development of local correlation techniques for measuring the proper motions of granules (November 1986; November & Simon 1988), it became possible to observe directly horizontal flows at the solar surface. For example, the existence of mesogranular convection, originally deduced from Dopplergrams of the vertical velocity (November et al. 1981), has been unambiguously confirmed by observations of ~6 Mm structures in horizontal flow and divergence maps derived from proper motion measurements (Title et al. 1986; Simon et al. 1988; November 1989). Subsequently it has been shown that the observed surface velocity fields resulting from supergranules, mesogranules, and exploding granules can be modeled surprisingly well by a collection of irrotational and axisymmetric velocity sources of varying sizes (Simon & Weiss 1989; Simon et al. 1991).

Recently, power spectra of the horizontal and vertical solar surface velocity fields have been estimated by analyzing spectra of the line-of-sight velocity fields in a series of 256″ × 240″ Doppler images displaced sequentially from the disk center (Chou et al. 1991, hereafter Paper I). The images were filtered in the frequency domain by excluding power with periods less than 12.8 minutes to eliminate *p*-mode contamination. Anomalous Doppler line shifts in regions of high magnetic field were also removed. With a 1″ image resolution the resultant power spectra span the range of wave numbers from $k \sim 0.042$ rad Mm^{-1} ($\lambda = 2\pi/k \sim 150$ Mm) to $k \sim 4.2$ rad Mm^{-1} ($\lambda \sim 1.5$ Mm) and easily include the scales corresponding to supergranules and mesogranules. When plotted on a log-log scale the power spectrum of the observable component of the horizontal velocity field (Fig. 7 of Paper I) can be characterized as generally decreasing in magnitude from $k \sim 0.1$ rad Mm^{-1} to $k \sim 4.0$ rad Mm^{-1} with a peak in the range $k \sim 0.135$–0.304 rad Mm^{-1} (corresponding to the supergranule length scale of ~30 Mm) and an average slope beyond the peak of ~ -1.64. A bend in the spectrum occurs at $k \sim 1.05$ rad Mm^{-1} ($\lambda \sim 6$ Mm), followed by a steeper decrease with slope ~ -4.0. Since they found no peak in the spectrum corresponding to the mesogranular length scale (~6 Mm), the authors concluded that "there is no evidence of apparent energy excess at the scale of mesogranulation," thereby contradicting the results from earlier Dopplergram and granule proper motion observations.

In this paper we show that the observed power spectra presented in Paper I are consistent with a distinct mesogranulation convection scale and, in fact, are just what we would reasonably expect from previously observed surface flow structures. We do this by extending the kinematic models of the convectively driven surface velocity fields (Simon & Weiss 1989; Simon et al. 1991) to include many supergranules and mesogranules covering a 300″ × 300″ area at the solar disk center (§ 2). To emulate closely the spatial resolution and field of view of Paper I's observations we project the observable component of the horizontal velocity field from the center of our model flow field onto a 256″ × 256″ observational plane with 1″ resolution. Computing the model power spectra we demonstrate good agreement with the shapes of the observed spectra of Paper I over ranges of the model parameters that are physically reasonable (§ 3). Comparing magnitudes of the model and observational spectra we find some nontrivial discrepancies which we discuss in § 4 along with our conclusions.

[1] Operated by the National Optical Astronomy Observatories for the Association of Universities for Research in Astronomy, Inc., under contract with the National Science Foundation. Partial support for the National Solar Observatory is provided by the USAF under a Memorandum of Understanding with the NSF.

2. MODEL OF CONVECTIVELY DRIVEN SURFACE FLOWS

The surface flow model is composed of a collection of independent velocity source functions distributed in an $x - y$ Cartesian coordinate system with each source function representing the contribution of a single supergranule or mesogranule convection cell. Simon & Weiss (1989) have shown that for each source, an irrotational velocity field v derived from a Gaussian velocity potential ϕ, where $v = -\nabla\phi$, is a good approximation to the observed horizontal velocity. We therefore choose a velocity potential of the form

$$\phi(x, y) = \sum_{i=1}^{N_s} \phi_i^s(x, y) + \sum_{j=1}^{N_m} \phi_j^m(x, y), \quad (1)$$

where N_s is the number of supergranules in the domain and N_m the number of mesogranules. The supergranule (s) and mesogranule (m) potential functions are given by

$$\phi_i^s(x, y) = \frac{V_s R_s}{2} \exp\left\{\frac{-[(x - x_i)^2 + (y - y_i)^2]}{R_s^2}\right\} \quad (2)$$

$$\phi_j^m(x, y) = \frac{V_m R_m}{2} \exp\left\{\frac{-[(x - x_j)^2 + (y - y_j)^2]}{R_m^2}\right\}, \quad (3)$$

where (V, R) determine the amplitude and spatial size of a velocity source, and (x_i, y_i) or (x_j, y_j) its center. Sizes of the N_s supergranules and N_m mesogranules are chosen to satisfy normal distributions of variances dR_s and dR_m about the average values $\langle R_s \rangle$ and $\langle R_m \rangle$, respectively. The normal distributions are slightly truncated by placing lower bounds $R_s^{\min}$ (supergranule) and $R_m^{\min}$ (mesogranule) on the source sizes. We do not include exploding granules in our model for two reasons: (1) the spectra of Paper I were filtered to exclude all power with variations less than 12.8 minutes, and this exceeds the lifetimes (~ 10 minutes) of most exploders (Title et al. 1989), and (2) the velocity field of a long-lived mesogranule closely approximates that of a collection of short-lived exploders normally distributed about the mesogranule center.

Ignoring curvature effects, we determine the position of the source centers on a 300″ × 300″ (218 Mm × 218 Mm) rectangular domain fixed to the solar surface in the following manner: imagine a uniform hexagonal grid covering the domain with nearest neighbor spacing d_s. A supergranule source is placed in each hexagonal cell with the center of the source (x_i, y_i) uniformly randomly distributed within a circle of radius ρ_s about the cell center. The centers of the N_m mesogranule sources (x_j, y_j) are uniformly randomly distributed over the entire domain with the average number of mesogranules per supergranule being N_{ms}, where $N_{ms} = N_m/N_s$. All source functions of a given variety are placed such that any two source centers are separated by at least a distance equivalent to their combined size. [We have also computed a normal distribution of N_{ms} mesogranules about each supergranule center. For variances of order $(d_s/2)^2$ the results of our analysis do not differ significantly from those results obtained assuming a uniform random distribution. Hence we consider only the latter distribution in the remainder of this paper].

To compare our model predictions with the observations of Paper I we compute from the velocity potential (eq. [1]) the observable component (v_{HO}) of the horizontal velocity (v_H), i.e., that component that would contribute to a line-of-sight Doppler velocity measurement:

$$v_{HO} = \frac{v \cdot (r - r_c)}{|r - r_c|}, \quad (4)$$

where $r = xe_x + ye_y$ and r_c is the location of the disk center as viewed from Earth, coincident with the domain center for the models presented here. We then project v_{HO} onto a 256″ × 256″ observational plane with 1″ resolution also spanned by an x-y Cartesian coordinate system.

In Figure 1 we show contour plots of v_{HO} in the observational plane corresponding both to an "idealized" regular

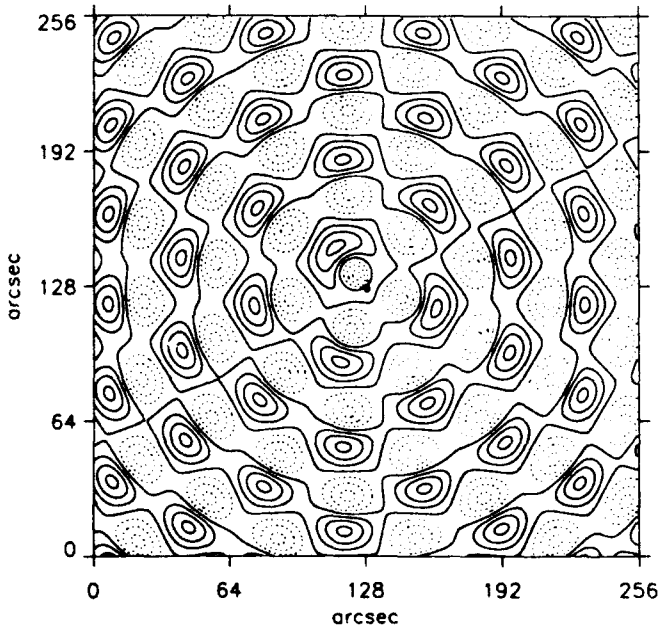

FIG. 1a

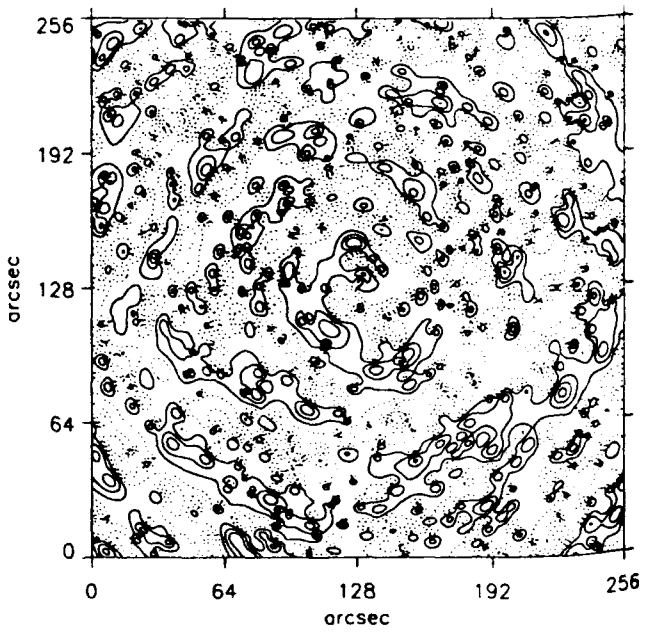

FIG. 1b

FIG. 1.—Contours of the observable component of the horizontal velocity field v_{HO} derived from the solar surface flow model in a 256″ × 256″ observational plane centered at the solar disk center showing (*a*) only supergranules in a regular hexagonal array and (*b*) a full complement of supergranules and mesogranules randomly distributed as described in § 2. Solid (dotted) lines represent positive (negative) values. See text for values of the model parameters.

array of identical supergranules (Fig. 1*a*) and the full "real" model with all scales and variations present (Fig. 1*b*). Figure 1*a* is generated with all the parameters set to zero except for $d_s = 40''$ (29 Mm), $V_s = 7.5 \times 10^{-2''}$ min^{-1} (0.91 km s^{-1}), and $\langle R_s \rangle = 12''$ (8.7 Mm). Figure 1*b* is generated with the same d_s, V_s, and $\langle R_s \rangle$ values and has $\rho_s = 15''$ (11 Mm), $dR_s = 5''$ (3.6 Mm), $R_s^{min} = 3''$ (2.2 Mm), $N_m = 12$, $V_m = 8.0 \times 10^{-2''}$ min^{-1} (0.97 km s^{-1}), $\langle R_m \rangle = 3''$ (2.2 Mm), $dR_m = 2''$ (1.5 Mm), and $R_m^{min} = 1''$ (0.73 Mm). Where possible, the parameters for the full model have been chosen to be consistent with values determined from proper motion measurements. In particular, V_s, $\langle R_s \rangle$, V_m, and $\langle R_m \rangle$ are close to values found in the measurements of Simon & Weiss (1989) and Simon et al. (1991). Further observational constraints imposed on the integrated power of the spectrum will be discussed in § 4.

3. MODEL POWER SPECTRA

Power spectra of the observable component of the horizontal velocity are constructed using the standard periodogram method (Press et al. 1986) generalized to two dimensions. Before Fourier transforming, a Hanning-type window function is applied to the spatial field in a 25" border region at the boundaries. Labeling the two-dimensional power spectrum as $P_{k_x k_y}$, where k_x and k_y are discrete wave vectors, the one-dimensional power spectrum P_k is defined as

$$P_k = \frac{1}{\Delta k} \sum_{k_y} \sum_{k_x} P_{k_x k_y} ,$$

$$k - \frac{\Delta k}{2} < (k_x^2 + k_y^2)^{1/2} \leq k + \frac{\Delta k}{2} , \qquad (5)$$

where $k = m\,\Delta k$, $m = 0, 1, 2, \ldots, 128$, and $\Delta k = 3.4 \times 10^{-2}$ rad Mm^{-1}.

We consider first a simple model comprised only of supergranule cells. Figure 2 displays three model power spectra corresponding to different values of the size distribution variance dR_s and maximum cell center offset ρ_s but with the common parameter values d_s, V_s, $\langle R_s \rangle$, and R_s^{min} from Figure 1*b*. It is clear that (*a*) if the supergranules are of uniform size ($dR_s = 0$) and fixed to the centers of the hexagonal lattice ($\rho_s = 0$), the spectrum is peaked in the range $k \sim 0.22$–0.29 rad Mm^{-1}. (*b*) Randomizing the positions of the supergranule centers ($\rho_s = 15''$) about the centers of the hexagonal lattice cells broadens this sharp peak. (*c*) Further broadening occurs when the sizes of the supergranules are distributed normally with a nonzero variance ($dR_s = 5''$) resulting in a spread of the peak power to smaller wavenumbers. In all three cases, however, the spectrum drops off sharply when $k > 0.5$ rad Mm^{-1} and is very different from the observed spectrum of Paper I (the dot-dash line superposed on Fig. 2) which is seen to have a clear shoulder at $k \sim 1.0$ rad Mm^{-1}. (Note that we also include as a dotted line the spectrum of Paper I scaled by a factor 0.13 so that it coincides more closely with the model spectra.)

The effect of adding mesogranule velocity sources into the model is illustrated in Figure 3. Three model power spectra are shown using the supergranule parameters and common mesogranule parameters N_m, V_m, $\langle R_m \rangle$, and R_m^{min} from Figure 1*b*, but with different values of the size distribution variance dR_m. Examining the power spectrum for mesogranules that are uniform in size ($dR_m = 0$, *solid line*), we see that the sharp decay for $k > 0.5$ rad Mm^{-1} that characterized the supergranule-only spectrum is replaced by a gentle mesogranular peak

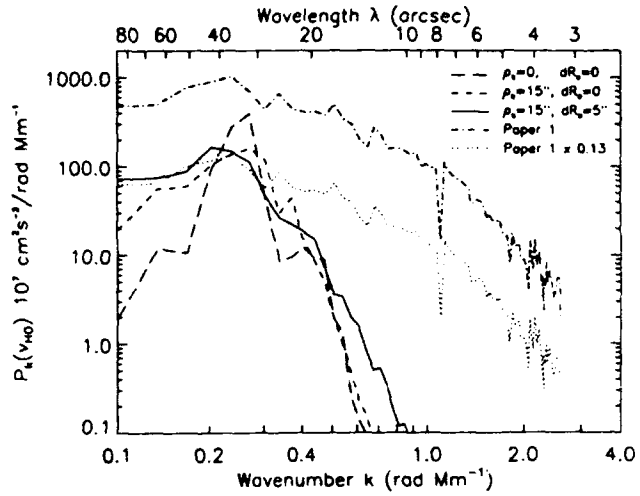

FIG. 2.—One-dimensional power spectra of the model velocity field v_{HO} for different values of the supergranule distribution parameters with no mesogranules present. The top axis shows the wavelength (λ) corresponding to the spectral wavenumber (k). See key and text for parameter values. For comparison we also show the spectrum of Paper I as published (*dot-dash line*) and when scaled by a factor 0.13 (*dotted line*).

between $k \sim 0.5$ rad Mm^{-1} and $k \sim 1.2$ rad Mm^{-1}. If we introduce a nonzero variance to the mesogranule size distribution ($dR_m = 1''.0$, *short dashed line*) the peak flattens into a "shelf" with a shoulder at $k \sim 1.0$ rad Mm^{-1}. Increasing the variance further ($dR_m = 2''.0$, *long dashed line*) steepens the mesogranular shelf and results in a log-log spectrum that decreases, on average, with a slope ~ -1.4 from the supergranule peak to the shoulder at $k \sim 1.0$ rad Mm^{-1}. Beyond the shoulder the slope steepens to ~ -4.3. This latter spectrum resembles closely the shape of the observed spectrum of Paper I (*dot-dash line*) and in addition matches satisfactorily the magnitude of the 0.13 scaled Paper I spectrum (*dotted line*).

All the power spectra displayed in Figures 2 and 3 have been computed from a specified configuration of supergranule and mesogranule velocity source functions with identical random

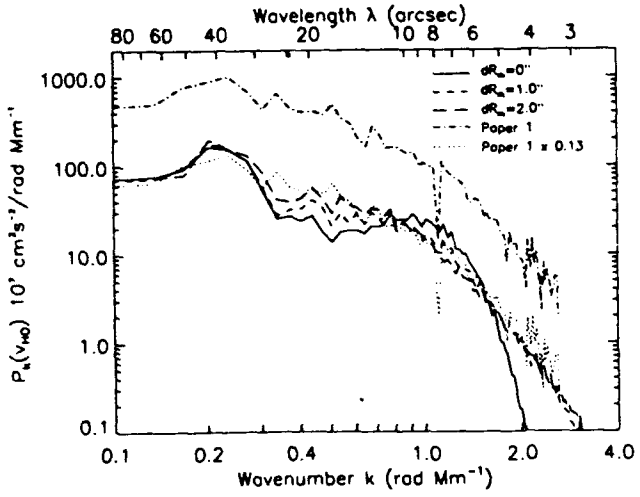

FIG. 3.—One-dimensional power spectra of the model velocity field v_{HO} for a fixed set of supergranule parameters but varying values of the mesogranule distribution parameters. See key and text for parameter values. The scaled and unscaled spectra from Paper I are also shown.

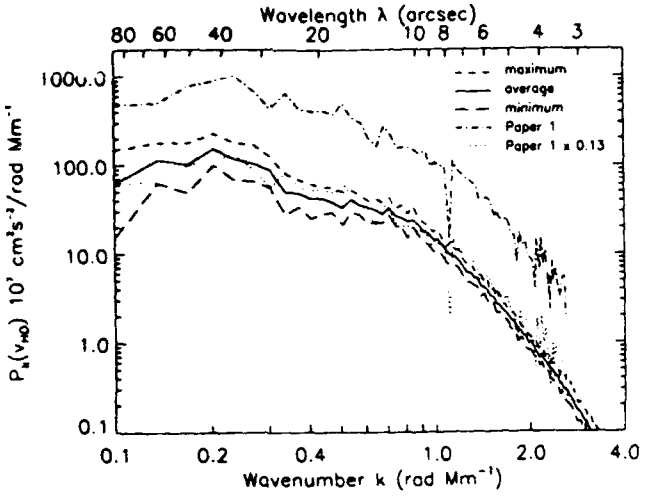

FIG. 4.—The average of the one-dimensional power spectra for the model velocity field v_{HO} (*solid line*) over 25 distinct configurations of the velocity source functions. The short-dashed line above and the long-dashed line below the average represent the maximum and minimum power, respectively, found at each k value in the 25 spectra. See text for values of the model parameters. Again we show the scaled and unscaled spectra from Paper I.

distributions of sizes and positions (except, of course, when the variance was zero). To estimate the statistical reliability of our model spectra, we used a random number generator to produce 25 different configurations with the same model parameters used for Figure 1*b*. From the power spectra for all these configurations we then determined the maximum, minimum, and average power for each discrete wavenumber bin and plotted the result in Figure 4. As before, we superpose the unscaled and scaled observational spectra from Paper I (*dot-dash*; *dotted lines*). The distance between the maximum curve (*short dashed line*) and minimum curve (*long dashed line*) is characteristic of the uncertainty in any power spectrum computed from a distinct configuration. Properties of the average power curve (*solid line*) are only slightly different from the distinct configuration shown in Figure 3. An essential point to note is that all model spectra in this parameter regime retain the signature of the mesogranule convection in the form of a shoulder at $k \sim 1.0$ rad Mm^{-1}.

4. DISCUSSION

Comparing the shape of the model spectra (Figs. 3 and 4) with the observational spectrum of Paper I we find qualitative agreement: at low k both spectra have a peak corresponding to the supergranule spacing that gives way to a decreasing function with relatively shallow slope interrupted by a bend at $k \sim 1.0$ rad Mm^{-1} followed by a more strongly decreasing function at higher k. Values of the logarithmic slopes and the locations in k of the supergranule peak and mesogranule break are in reasonable agreement given the statistical deviations of the model and the experimental uncertainties of the observations.

However, comparing the magnitude of the model spectrum with the observational spectrum of Paper I we find a considerable discrepancy. For each k the power in the observational spectrum is 7–8 times larger than that of the model spectrum (Fig. 3). In our model, the parameters have not been chosen simply to fit the shape of the observed spectrum, but rather to be consistent with the parameter values determined from proper motion measurements. An additional constraint on the model is the estimate of the magnitude of the horizontal velocity field derived from spatially averaged Doppler velocity observations (Hart 1956; Simon & Leighton 1964; Giovanelli 1980). By Parseval's theorem, the integrated power spectrum is equal to the mean square amplitude $\langle v_{HO}^2 \rangle$, where the average is over the entire spatial domain. Integrating the average power spectrum of Figure 4 we find an rms observable component of the horizontal velocity $\langle v_{HO}^2 \rangle^{1/2} \approx 0.23$ km s^{-1}. Converting this to the peak horizontal velocity v_H by multiplying by a factor of 2 (Giovanelli 1980) we obtain $v_H \approx 0.46$ km s^{-1}, a value consistent with the 0.3–0.5 km s^{-1} determined from spatially averaged Doppler velocity observations.

We therefore believe that the discrepancy between the model and observational spectra lies in the data analysis performed in Paper I. We have discussed with the authors of Paper I their inconsistent labeling of graphs (Chou 1991), confusion of the horizontal velocity with observable component of the horizontal velocity (Chou 1991), and the absence of any explicit references to the applied window functions (Chou 1991) in the power spectrum decomposition analysis. These problems make it impossible for us to reproduce the power spectrum of the observable component of the horizontal velocity field (Fig. 6 of Paper I) from the power spectra of the Doppler velocities on different patches of the solar surface (Fig. 2 of Paper I). We assume that the power spectrum shown in Figure 6 of Paper I is as labeled; i.e., the power spectrum of the velocity function defined in equation (A2) of Paper I. If we estimate the rms velocity associated with the supergranule peak by taking the square root of the sum of the power in the wavenumber range $k \sim 0.14$–0.30 rad Mm^{-1} (Parseval's theorem), we then find $\langle v_{HO}^2 \rangle^{1/2} \sim 0.35$ km s^{-1} corresponding to a peak velocity $v_H \sim 0.7$ km s^{-1}. This number is already larger than the value determined by earlier Doppler velocity measurements. The discrepancy is made considerably worse by the realization that a true comparison requires the integration of the power spectrum to wavenumbers characteristic of the resolution of the Doppler measurements; namely, to values $k \geq 1.0$ rad Mm^{-1}.

In summary, we have shown in this paper that a model composed of both supergranule and mesogranule convective surface flows produces a power spectrum of the azimuthal component of the horizontal velocity that is consistent with the shape of the observed spectrum reported in Paper I. We believe that discrepancies in the relative magnitudes of the model and observed spectra arise from errors in the analysis of Paper I. We caution that our model is not unique in being able to reproduce the specific shape of the observed spectrum, and we do not claim to have isolated the optimal set of parameters most characteristic of the physical processes involved in solar convection. Rather, we have determined a set of parameters for supergranule and mesogranule flows that is consistent with (1) spatially averaged Doppler velocity observations, (2) proper motion measurements of the granulation, and (3) (with the caveats discussed above) the power spectra of Paper I. We conclude, therefore, that the spectra of Paper I do indeed show the presence of energy at the scale of the mesogranules, and we disagree strongly with the authors' assertion to the contrary.

We wish to thank Steve Keil, Larry November, and Nigel Weiss for helpful discussions.

REFERENCES

Chou, D.-Y., LaBonte, B. J., Braun, D. C., & Duvall, T. L., Jr. 1991, ApJ, 372, 314 (Paper I)
Chou, D.-Y. 1991, personal communication
Giovanelli, R. G. 1980, Solar Phys., 67, 211
Hart, A. B. 1956, MNRAS, 116, 38
November, L. J. 1986, Appl. Optics, 25, 392
———. 1989, ApJ, 344, 494
November, L. J., & Simon, G. W. 1988, ApJ, 333, 427
November, L. J., Toomre, J., Gebbie, K. B., & Simon, G. W. 1981, ApJ, 245, L123
Press, W. H., Flannery, B. P., Teukolsky, S. A., & Vetterling, W. T. 1986, in Numerical Recipes (Cambridge: Cambridge Univ. Press), Chap. 12
Simon, G. W., & Leighton, R. B. 1964, ApJ, 140, 1120
Simon, G. W., Title, A. M., Topka, K. P., Tarbell, T. D., Shine, R. A., Ferguson, S. H., Zirin, H., & the SOUP Team 1988, ApJ, 327, 964
Simon, G. W., & Weiss, N. O. 1989, ApJ, 345, 1060
Simon, G. W., Title, A. M., & Weiss, N. O. 1991, ApJ, 375, 775
Title, A. M., Tarbell, T. D., Simon, G. W., & the SOUP Team 1986, Adv. Space Res., 6, 253
Title, A. M., Tarbell, T. D., Topka, K. P., Ferguson, S. H., Shine, R. A., & the SOUP Team 1989, ApJ, 336, 475